Evidence for a Nodal Energy Gap in the Iron-Pnictide Superconductor LaFePO from Penetration Depth Measurements by Scanning SQUID Susceptometry

Clifford W. Hicks,[1] Thomas M. Lippman,[1] Martin E. Huber,[2] James G. Analytis,[1] Jiun-Haw Chu,[1] Ann S. Erickson,[1] Ian R. Fisher,[1] and Kathryn A. Moler[1]

[1]*Geballe Laboratory for Advanced Materials, Stanford University, Stanford, California, 94305, USA and Stanford Institute for Materials and Energy Sciences, SLAC National Accelerator Laboratory, 2575 Sand Hill Road, Menlo Park, California 94025, USA*

[2]*Departments of Physics and Electrical Engineering, University of Colorado Denver, Denver, Colorado, 80217, USA*

(Received 1 April 2009; published 18 September 2009)

We measure changes in the penetration depth λ of the $T_c \approx 6$ K superconductor LaFePO. In the process, scanning SQUID susceptometry is demonstrated as a technique for accurately measuring *local* temperature-dependent changes in λ, ideal for studying early or difficult-to-grow materials. λ is found to vary linearly with temperatures from 0.36 to ~2 K, with a slope of 143 ± 15 Å/K, suggesting line nodes in the superconducting order parameter. The linear dependence up to $\sim T_c/3$, similar to the cuprate superconductors, indicates well-developed nodes.

DOI: 10.1103/PhysRevLett.103.127003 PACS numbers: 74.25.Nf, 74.20.Rp

Research on the iron pnictide superconductors has been intense. Most attention has focused on arsenic-based materials, which have the highest transition temperatures, but most of which only superconduct at ambient pressure when doped, resulting in intrinsic disorder. Superconductivity in polycrystalline LaFePO was announced in 2006 [1], and in single crystals in 2008 [2,3], with $T_c \approx 6$ K. Crystals with residual resistivity ratios $\rho(300\ \mathrm{K})/\rho(0)$ as high as 85 [3] make LaFePO a clean system which may prove a good model of the higher-T_c arsenide compounds: although not showing the magnetic order found in the arsenide compounds, its electronic structure is very similar [4]. The crystals in this study were grown in tin flux, using La_2O_3 as a precursor material, which appears to result in generally higher residual resistivity ratio and ~1/2 K lower T_c than Fe_2O_3-based growths [2,3]; details of the synthesis are given in Ref. [3].

The temperature dependence of λ provides information on the superconducting order parameter (OP). OPs with line nodes result in a T-linear dependence of $\Delta\lambda(T) \equiv \lambda(T) - \lambda(0)$ at low T [5]. Scattering can modify this dependence to T^2 [6]. A fully gapped OP results in $\Delta\lambda \propto T^{-1/2}\exp(-T_0/T)$ [7]. For the iron pnictide superconductors, proposed OPs include nodal and nodeless s [8,9], $s + d$ [10], p [11,12], and d [9,12,13]. Most of these predictions are based on calculations in an unfolded, 1 Fe per unit cell Brillouin zone, neglecting the spin-orbit-coupling-induced avoided crossings between the electron pockets in the true zone [4], which would alter the nodal structure of some of the proposed OPs. It is also a possibility that different pnictide superconductors, although electronically similar, have different OPs [14].

Radio-frequency tunnel diode resonator and microwave cavity perturbation measurements on iron arsenide superconductors have shown both power-law and exponential $\Delta\lambda(T)$. Power-law dependence has been found in $Ba(Fe_{1-x}Co_x)_2As_2$ [15], with the exponent n varying between 2.0 and 2.6 with doping. $n \approx 2$ has been found in $Ba_{1-x}K_xFe_2As_2$ [16], $NdFeAsO_{0.9}F_{0.1}$ [17], and $LaFeAsO_{0.9}F_{0.1}$ [17]. Exponential behavior has been found in $Ba_{1-x}K_xFe_2As_2$ [18], $PrFeAsO_{1-y}$ [19], and $SmFeAsO_{0.8}F_{0.2}$ [20].

In LaFePO, Fletcher *et al.* found nearly linear $\Delta\lambda(T)$ to below 150 mK [21], using a radio-frequency tunnel diode circuit. However, early LaFePO samples have had irregular shapes, which complicate rf and microwave measurements: to isolate λ_{ab}, the magnetic field of the excitation must be specifically oriented relative to the crystal axes, and frequently knowledge of the sample size is necessary to obtain the correct value of $\Delta\lambda$. Fletcher *et al* report these slopes $d\lambda/dT$ on three samples: 412, 436, and 265 Å/K (over $0.7 < T < 1.0$ K). The magnitude of $d\lambda/dT$ constrains the number and opening angle of nodes, so confirmation with additional measurement is desirable.

Scanning SQUID susceptometry has been used to observe superconducting transitions [22] and to determine the Pearl length Λ of thin superconducting films, for $\Lambda \sim$ 10–100 μm [23]. We extend this technique to measurement of nm-scale changes in local λ with varying sample temperature. Our susceptometer is a niobium-based design [24]; its front end is shown in Fig. 1. The pickup loop is part of a SQUID. An excitation current (here at 1071 Hz) is applied to the field coil to measure the mutual inductance M between the field coil and pickup loop. The susceptometer chip is polished to a point, aligned at an angle (here ≈16°) to the sample, and mounted onto a 3-axis scanner. The Meissner response of superconducting samples partially shields the field coil, so M decreases as the susceptometer approaches the sample. In typical measurements, the excitation current gives a $\sim 10^{-4}$ T field at the superconductor surface.

 © 2009 The American Physical Society

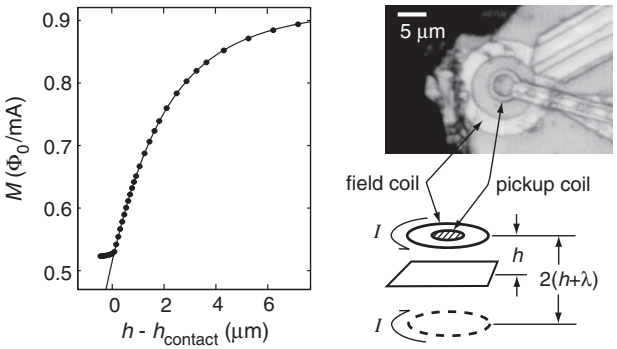

FIG. 1. Left: Field coil-pickup loop mutual inductance M against height above the sample; h_{contact} is the height at which the corner of the susceptometer chip contacts the sample. The line is a fit of Eq. (1). Right: photograph of the front end of the susceptometer and schematic of the susceptometer-sample geometry. The dashed loop is the image field coil.

To model the susceptometry (Fig. 1), the field coil is taken as a loop of radius R at a height h above the superconductor surface, and the superconductor response field as an image coil placed a height $2h_{\mathrm{eff}}$ beneath the field coil, where the effective height $h_{\mathrm{eff}} \equiv h + \lambda$. The flux through the pickup coil (radius a) is taken as the field at its center times its area. All coils are taken parallel to the surface, neglecting the alignment angle. These approximations give

$$M = \frac{\mu_0}{2}\pi a^2\left(\frac{1}{R} - \frac{R^2}{(R^2 + 4h_{\mathrm{eff}}^2)^{3/2}}\right). \quad (1)$$

To measure changes in λ, the susceptometer is placed in contact with a flat ab-plane area of the sample, and the sample temperature T is varied. The contact force is chosen to be sufficient to overcome system vibration but weak enough to avoid excessive thermal coupling. (The susceptometer is maintained at ≈ 0.3 K as the sample is heated.) The contact keeps h constant at h_{contact} (≈ 3 μm, set by the alignment angle), so changes to h_{eff} are changes in λ_{ab}: for $h \gg \lambda$, the response field of the superconductor is a function of h_{eff} alone [25]. Thus, the physical origin of Eq. (1) is irrelevant as long as it accurately models the dependence of M on h, which Fig. 1 shows to be the case. R and a are fitting parameters obtained separately for each sample; they approximately match the actual dimensions of the susceptometer, but their precise values vary with alignment angle and sample surface orientation. Crucial to measurement of $\Delta\lambda$, if the susceptometer is over a flat ab surface and $\lambda_a = \lambda_b$, then the relevant penetration depth is λ_{ab} alone, even with nonzero alignment angle [25].

What is the accuracy of measurement of $\Delta\lambda$? The fit to Eq. (1) returns R and a consistent with a particular conversion constant, in μm/V, between h and the voltage applied to the scanner, which is measured separately, here with $\pm 5\%$ accuracy. So there is $\pm 5\%$ systematic error on all $\Delta\lambda$ in this work. Also, deviations from the fit give errors up to 1.5%. At large λ, such that $\lambda \sim h$, the assumption that the response field is a function of $h + \lambda$ breaks down; numerical simulation shows that, at $h = 3$ μm and $\lambda(0) = 5000$ Å, this assumption leads $\Delta\lambda$ to be underestimated by 1% at $\Delta\lambda = 5000$ Å and 4% at 10 000 Å. Thermal gradients from the susceptometer-sample contact have minimal effect: control tests on sapphire show that the change in h_{eff} attributable to these gradients is no more than ~ 20 Å for T varying between 1 and 8 K. By tracking T_c of LaFePO, we determine that contact locally cools the sample by only ~ 40 mK at $T = 6$ K.

As a test, we measure the penetration depth of a lump of industrial-grade lead (Fig. 2). A ~ 100 Å-scale downward drift of h_{eff}, due to the sensor tip gradually polishing the soft lead surface, is subtracted from our data. The drift rate is T-independent and was measured separately from the data in Fig. 2, so the flatness of $\Delta\lambda$ at low T is real.

Figure 3 shows the main result of this work: $\Delta\lambda_{ab}$ vs T for two LaFePO crystals [at the points indicated in Figs. 4(e) and 4(f)]. For each data set, $\Delta\lambda$ was recorded over multiple temperature sweeps, both warming and cooling, and found to follow the same path. λ is seen to vary nearly linearly with temperature. Fitting $\Delta\lambda = A + BT^n$ over $0.7 < T < 1.6$ K, from top to bottom $n = 1.22(4)$, 1.13(10), and 0.97(5) are obtained for the three curves in Fig. 3(a).

Photographs of the two LaFePO specimens are shown in Fig. 4. A susceptibility scan (a scan of the spatial variation in M) is shown in Fig. 4(c). M varies strongly with h, so features in individual scans mainly reflect surface topography. More useful is comparison of scans at different T. Figure 4(d) shows a map of $h_{\mathrm{eff}}(3\ \mathrm{K}) - h_{\mathrm{eff}}(0.4\ \mathrm{K})$ on sample #2, which reveals two useful observations. (1) Where the sample surface is not flat, λ_c mixes in strongly and Δh_{eff} is large; one needs to be at least ~ 10 μm from an edge to measure λ_{ab}. (2) Where the

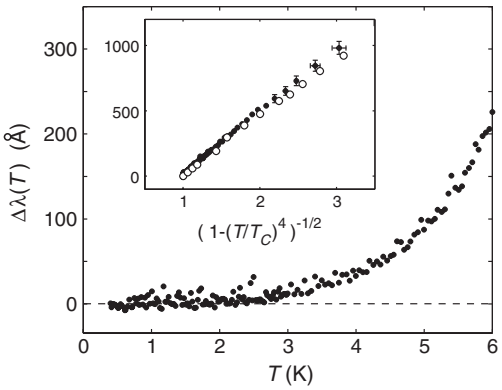

FIG. 2. $\Delta\lambda(T) \equiv \lambda(T) - \lambda(0)$ of Pb. A drift has been subtracted as described in the text. Inset: Open symbols: measurement of Gasparovic and McLean [29]. Filled symbols: present data; the vertical error bars are the systematic $\pm 5\%$ error on all $\Delta\lambda$ data in this Letter.

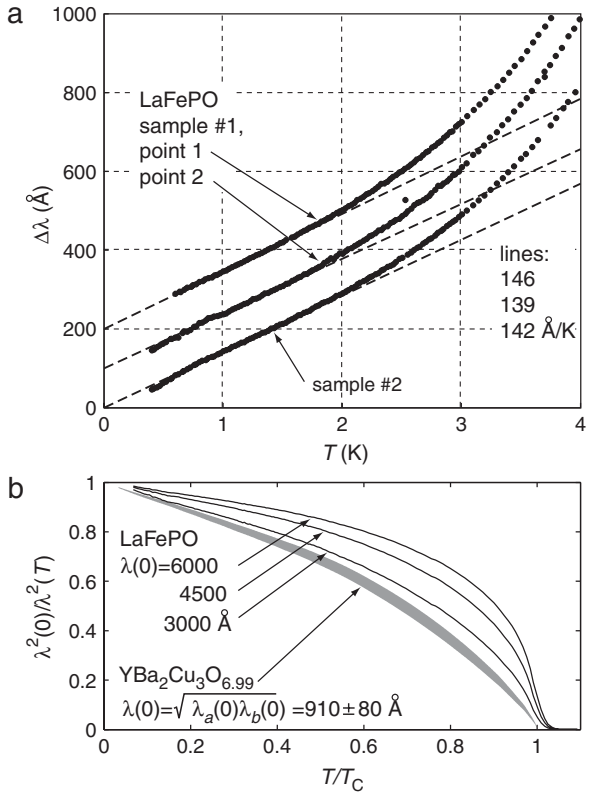

FIG. 3. Top: $\Delta\lambda$ of two LaFePO specimens, at the points indicated in Fig. 4. The lines were fit over $0.7 < T < 1.6$ K. Bottom: black lines are possible superfluid densities for LaFePO sample #1, point 2, with different $\lambda(0)$. Shaded area: superfluid density of $YBa_2Cu_3O_{6.99}$ $[1/(\lambda_a\lambda_b)]$, from [30,31]; the width of the shaded area reflects uncertainty in $\lambda(0)$.

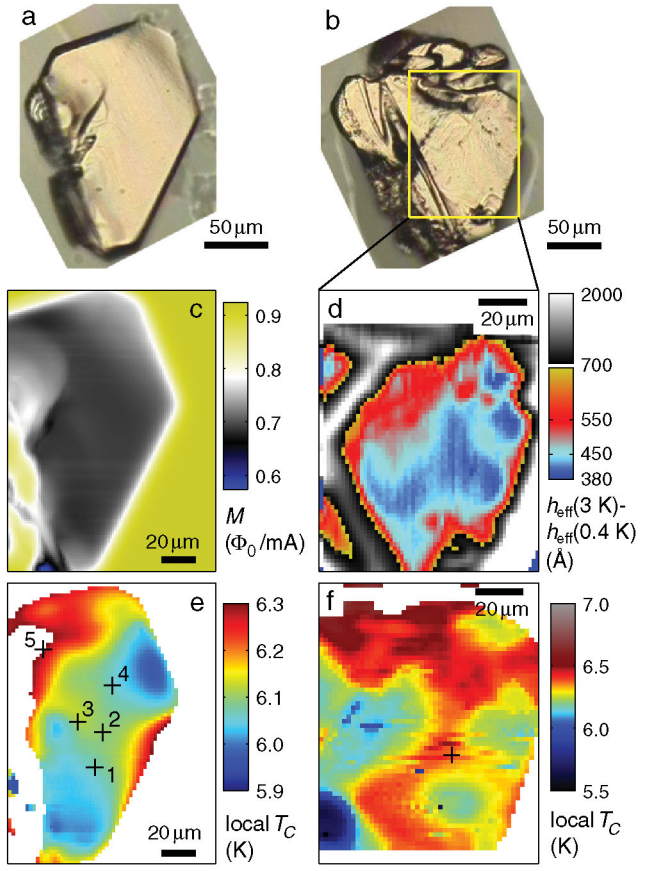

FIG. 4 (color). (a), (b) LaFePO specimens #1 and #2. (c) Susceptibility scan of #1 at $T = 0.4$ K. Over the superconductor M is reduced from its vacuum level by the Meissner response. (d) Change in $h_{\rm eff} = h + \lambda$ between 0.4 and 3 K over specimen #2. (e), (f) Maps of local T_c, over the same areas as in (c) and (d). The crosses indicate the points where $\Delta\lambda(T)$ data were collected.

sample is flat, and $\Delta h_{\rm eff} = \Delta\lambda_{ab}$, $\Delta\lambda_{ab}$ is homogeneous to within ~5%; areas of moderately increased $\Delta h_{\rm eff}$ are areas where the surface was found to be pitted.

Maps of local T_c, shown in Figs. 4(e) and 4(f), are made by performing susceptibility scans at various T and extracting $\Delta h_{\rm eff}(T)$. Over most of both samples, weak tails of superfluid density persist to a few 0.1 K above the dominant local T_c (and in places beyond 7 K), giving uncertainty to estimates of T_c. To determine local T_c, $\Delta h_{\rm eff}$ is taken as $\Delta\lambda$, and the $\lambda_{ab}(0) = 4500$ Å curve in Fig. 3(b) is taken as a reference. The local $\lambda(0)$ (which varies with topography) and T_c are varied to obtain the best match to the reference. Varying the reference $\lambda_{ab}(0)$ by 1000 Å varies the calculated T_c's by ~0.1 K.

$\lambda(0)$ could in principle be extracted from the geometry of the susceptometer and sample, but the uncertainties are large. From the variation of M with surface orientation and SEM images of the susceptometer, a plausible contact point on the susceptometer can be identified, and comparison with the lead specimen indicates that $\lambda_{ab}(0)$ of LaFePO likely falls in the range 3500–5500 Å.

At the five points on sample #1 indicated in Fig. 4(e), $d\lambda/dT$ measured over $0.8 < T < 1.6$ K is 146, 139, 136, 150, and 205 Å/K, and at the single measurement point on sample #2, 142 Å/K. The 205 Å/K measurement was at a point with significant topography and can be excluded. With the 5% and 1.5% uncertainties, $d\lambda/dT$ is 143 ± 15 Å/K.

In plots of the superfluid density, the T-linear portion at low T extends to a similar fraction of T_c in LaFePO as $YBa_2Cu_3O_{6.99}$ [Fig. 3(b)], indicating that the nodes are similarly deep. In contrast, accidental nodes in nodal s OP proposals could result in shallow, accidental nodes [26]. Also apparent in Fig. 3 is that the superfluid density of LaFePO falls sharply just below T_c. [This feature is more pronounced taking large $\lambda(0)$, but present for $\lambda(0)$ as low as 1800 Å.] If the pairing is mediated by magnetic fluctuations of the conduction electrons themselves, then such a sharp drop may result from a gapping-out of low-frequency, pair-breaking fluctuations [27].

Fits of a single-band d-wave model, following Ref. [28], to the superfluid density perform reasonably well, although

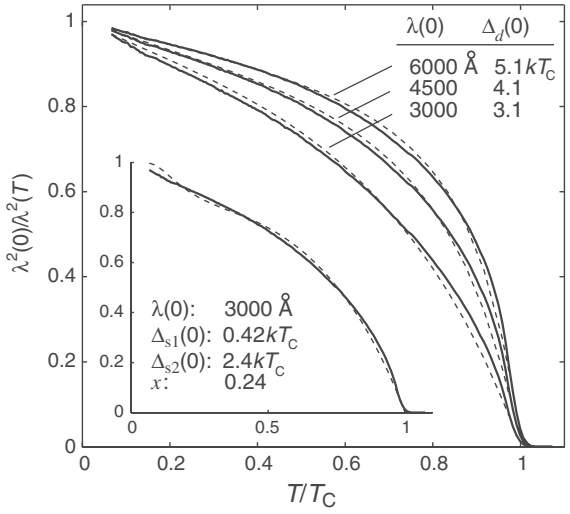

FIG. 5. Solid lines: superfluid density of LaFePO. Dashed lines: fits. Main panel: single-band d-wave model, with the indicated guesses for $\lambda(0)$ and resulting fitting parameter $\Delta_d(0)$. Inset: two-band s-wave model, taking $\lambda(0) = 3000$ Å, with the fitting parameters.

they miss the steepness of the drop near T_c (Fig. 5). The gap in the fits is assumed to follow the weak-coupling BCS temperature dependence (as approximated by Eq. 18 of Ref. [28], with the parameter $a = 4/3$). To further constrain the OP, measurement of $\lambda(0)$ and Δ will be necessary. A fit of a two-band s-wave model, where the superfluid density $\rho_s(T) = x\rho_1(T) + (1 - x)\rho_2(T)$, with ρ_1 and ρ_2 the superfluid densities of bands with gaps Δ_{s1} and Δ_{s2} (that also each follow the weak-coupling BCS T dependence), fails to capture the linear T dependence at low T.

In conclusion, we have observed a linear temperature dependence of $\Delta\lambda_{ab}(T)$ below $\sim T_c/3$ in LaFePO and measured its slope, 143 ± 15 Å/K, using a local technique.

This work was funded by the United States Department of Energy (DE-AC02-76SF00515). We thank Douglas Scalapino, John Kirtley, David Broun, Vladimir Kogan, and Walter Hardy for useful discussions.

[1] Y. Kamihara *et al.*, J. Am. Chem. Soc. **128**, 10012 (2006).
[2] J. J. Hamlin, R. E. Baumbach, D. A. Zocco, T. A. Sayles, and M. B. Maple, J. Phys. Condens. Matter **20**, 365220 (2008).
[3] J. G. Analytis *et al.*, arXiv:cond-mat/08105368.
[4] A. I. Coldea *et al.*, Phys. Rev. Lett. **101**, 216402 (2008); A. Carrington *et al.*, Physica C (Amsterdam) **469**, 459 (2009).
[5] J. Annett, N. Goldenfeld, and S. R. Renn, Phys. Rev. B **43**, 2778 (1991).
[6] P. J. Hirschfeld and N. Goldenfeld, Phys. Rev. B **48**, 4219 (1993).
[7] M. Tinkham, *Introduction to Superconductivity* (McGraw-Hill, New York, 1996), 2nd ed.
[8] I. I. Mazin, D. J. Singh, M. D. Johannes, and M. H. Du, Phys. Rev. Lett. **101**, 057003 (2008); Fa Wang, Hui Zhai, Ying Ran, A. Vishwanath, and D. H. Lee, Phys. Rev. Lett. **102**, 047005 (2009); W. Q. Chen, K. Y. Yang, Yi Zhou, and F. C. Zhang, Phys. Rev. Lett. **102**, 047006 (2009); A. V. Chubukov, D. V. Efremov, and I. Eremin, Phys. Rev. B **78**, 134512 (2008).
[9] K. Kuroki *et al.*, Phys. Rev. Lett. **101**, 087004 (2008).
[10] Kangjun Seo, B. A. Bernevig, and Jiangping Hu, Phys. Rev. Lett. **101**, 206404 (2008).
[11] P. A. Lee and X. G. Wen, Phys. Rev. B **78**, 144517 (2008).
[12] X. L. Qi, S. Raghu, C. X. Liu, D. J. Scalapino, and S. C. Zhang, arXiv:cond-mat/08044332.
[13] Q. M. Si and E. Abrahams, Phys. Rev. Lett. **101**, 076401 (2008); Z. J. Yao, J. X. Li, and Z. D. Wang, New J. Phys. **11**, 025009 (2009).
[14] S. Graser, T. A. Maier, P. J. Hirshfeld, and D. J. Scalapino, New J. Phys. **11**, 025016 (2009).
[15] R. T. Gordon *et al.*, Phys. Rev. B **79**, 100506(R) (2009); R. T. Gordon *et al.*, Phys. Rev. Lett. **102**, 127004 (2009).
[16] C. Martin *et al.*, Phys. Rev. B **80**, 020501(R) (2009).
[17] C. Martin *et al.*, Phys. Rev. Lett. **102**, 247002 (2009).
[18] K. Hashimoto *et al.*, Phys. Rev. Lett. **102**, 207001 (2009).
[19] K. Hashimoto *et al.*, Phys. Rev. Lett. **102**, 017002 (2009).
[20] L. Malone *et al.*, Phys. Rev. B **79**, 140501(R) (2009).
[21] J. D. Fletcher *et al.*, Phys. Rev. Lett. **102**, 147001 (2009).
[22] B. W. Gardner *et al.*, Rev. Sci. Instrum. **72**, 2361 (2001).
[23] F. Tafuri, J. R. Kirtley, P. G. Medaglia, P. Orgiani, and G. Balestrino, Phys. Rev. Lett. **92**, 157006 (2004).
[24] M. E. Huber *et al.*, Rev. Sci. Instrum. **79**, 053704 (2008).
[25] V. G. Kogan, Phys. Rev. B **68**, 104511 (2003).
[26] V. Mishra *et al.*, Phys. Rev. B **79**, 094512 (2009).
[27] P. Monthoux and D. J. Scalapino, Phys. Rev. B **50**, 10339 (1994).
[28] R. Prozorov and R. W. Giannetta, Supercond. Sci. Technol. **19**, R41 (2006).
[29] R. F. Gasparovic and W. L. McLean, Phys. Rev. B **2**, 2519 (1970).
[30] D. A. Bonn and W. N. Hardy, in *Handbook of High-Temperature Superconductivity*, edited by J. R. Schrieffer (Springer, New York, 2007).
[31] T. Pereg-Barnea *et al.*, Phys. Rev. B **69**, 184513 (2004).